Polymer Degradation and Stability 121 (2015) 407–419

Contents lists available at ScienceDirect

Polymer Degradation and Stability

journal homepage: www.elsevier.com/locate/polydegstab

Moisture uptake characteristics of a pultruded fibre reinforced polymer flat sheet subjected to hot/wet aging

S.A. Grammatikos [a, b, *], B. Zafari [c], M.C. Evernden [a, b], J.T. Mottram [c], J.M. Mitchels [d]

[a] BRE Centre for Innovative Construction Materials, United Kingdom
[b] Department of Architecture and Civil Engineering, University of Bath, Bath BA2 7AY, United Kingdom
[c] Civil Research Group, School of Engineering, University of Warwick, Coventry CV4 7AL, United Kingdom
[d] Department of Chemistry, University of Bath, Bath BA2 7AY, United Kingdom

ARTICLE INFO

Article history:
Received 29 April 2015
Received in revised form
19 August 2015
Accepted 7 October 2015
Available online 22 October 2015

Keywords:
Pultruded FRP
Moisture uptake
Fickian theory
Diffusion coefficient
Infrared Spectroscopy
Scanning electron microscopy

ABSTRACT

This paper studies the moisture uptake characteristics of a pultruded E-glass fibre reinforced (isophthalic polyester) polymer after long-term exposure to hot/wet conditions. Both fully exposed samples of varying aspect ratios and selectively exposed samples were immersed in distilled water at 25 °C, 40 °C, 60 °C and 80 °C for a period of 224 days. For the fully exposed condition, bulk and directional diffusion coefficient values were determined. A three-dimensional approach using Fickian theory was applied to approximate the principal direction diffusions at 60 °C by using mass changes from samples having different aspect ratios. This revealed that the diffusion coefficient in the longitudinal (pultrusion) direction to be an order of magnitude higher than in the transverse and through-thickness principal directions. Diffusion coefficients in the three principal directions have also been determined for the selectively exposed condition at 60 °C through the application of one-dimensional Fickian theory. It was found that the size and shape of the samples influences moisture uptake characteristics, and thereby the values determined for bulk and directional diffusion coefficients. Furthermore, the influence of exposure temperature on moisture uptake and mass loss with time was examined. Investigation of the water medium by means of electrical measurements suggested that decomposition of the polymeric composite initiates very early, even after the very first day of immersion. Comparison between the infrared signatures from the pultruded material and the water's residual substances revealed significant decomposition, and this behaviour is verified by Fourier Transform Infrared Spectroscopy (FTIR), Scanning Electron Microscopy (SEM) and Energy Dispersive Spectroscopic (EDS) analysis as well as the recorded mass loss after 224 days of aging.

1. Introduction

The eagerness for low-cost, high performance and lightweight engineering structures has led to the promotion of Fibre Reinforced Polymer (FRP) composites [1]. In particular, Pultruded FRP (PFRP) shapes and systems are being increasingly used in aerospace, civil and naval engineering applications. They commonly consist of E-glass fibre reinforcement (layers of unidirectional rovings and continuous filament mats) in a thermoset (e.g. polyester or vinylester) resin based matrix. PFRP material has a density about one quarter of steel. Longitudinal tensile strength can be over 200 N/mm^2 and comparable with structural grade steel. The longitudinal modulus of elasticity, at 12–30 kN/mm^2, is up to 17 times lower, whereas the modulus of elasticity perpendicular to the direction of pultrusion is one-quarter to one-third of the longitudinal value. Shear properties are also matrix governed with in-plane strength of 30–80 N/mm^2 and in-plane modulus of 3–5 kN/mm^2. One of the advantages of this construction material over conventional materials is that it is corrosion-resistant in relatively aggressive environments, such as found in aqueous mediums. PFRPs shapes and systems are being extensively considered for primary and secondary structural elements in civil engineering works [2]. The environmental service conditions in any field applications may affect the material's intrinsic structural properties, increasing the probability of failure before the end of the structure's service life. Generally, civil engineering structures are designed for a working

* Corresponding author. Department of Architecture and Civil Engineering, University of Bath, Bath BA2 7AY, United Kingdom.
E-mail address: grammatikos@outlook.com (S.A. Grammatikos).

http://dx.doi.org/10.1016/j.polymdegradstab.2015.10.001

life of more than 50 years, ideally with minimal maintenance [3]. Long-term property retention is of critical importance to engineers when managing assets and planning for their routine inspection and maintenance. Due to the hydrophilic nature of both the E-glass fibres and the polymer matrix (e.g. due to the ester-end groups), moisture uptake into FRPs is a crucial phenomenon when determining material deterioration and time varying mechanical properties for structural engineering [4]. A thorough investigation into the mechanisms which lead to environmental aging is essential if we are to have reliable and safe designs [5–7].

Understanding how moisture affects the durability, and long-term mechanical property retention, in aggressive environments has to be a prerequisite before any FRP can be qualified as an engineering material [2,8]. At most civil engineering sites the service environment involves, in combination with other actions, the presence of moisture in various forms. Prolonged exposure to moist environments results in both reversible and irreversible internal material changes. Reversible changes are said to be physical, and will recover when the FRP is dried. Physical aging involves changes in the mechanical properties and volume as material swells from the water ingress [9]. Swelling is the resistive reaction to hygrothermal exposure and causes changes in residual stresses. Chemical degradation is irreversible and induces property changes in the polymer matrix, fibre reinforcement, as well as the fibre/matrix interface. Typically, it has been established that the polymer matrix is more prone to damage than the fibre reinforcement [2]. Chain scission, residual cross-linking, hydrolysis, oxidation and plasticization are known major effects of moisture concentration in the polymer [10]. Furthermore, when moisture penetrates throughout the FRP, it may attack the E-glass fibres in the form of stress corrosion, leading to overall deterioration of mechanical properties [11]. The fibre/matrix interface is the crucial component that couples the matrix with the fibres. This constituent is susceptible to chemical degradation in the presence of moisture, which reduces the adhesion [12,13] and enhances interfacial capillary (or wicking) action by exposing the reinforcement surface for the promotion of fibre degradation. It is known that the performance of the interface is always dependent on the chemical, physical and mechanical interaction between fibres and the polymer matrix. Matrix plasticization and interface failures are reported to be the most effective in reducing the bulk mechanical performance [8]. In all situations, it is evident that water ingress has a negative effect on mechanical properties, either by instigating or speeding up the evolution of various forms of internal degradation/damage. Upon moisture uptake, H_2O molecules may either diffuse through the polymeric structure's inherent micro-voids (called 'free volume' or 'free space') and any present porosity or micro-cracks (i.e. from matrix shrinkage after curing), or travel via a capillary phenomenon along the fibre/matrix interfacial regions [7,14]. 'Free volume' or 'free space' refers to the unfilled voiding in a polymer structure that is not occupied by polymer molecules and is the subtraction of the total measured volume of the polymer by the actual volume that is 'filled' with polymer molecules [9].

Long-term exposure in hot/wet conditions has been employed by many researchers [7,15,16] as a means of accelerating aging in order to obtain characterization test results that can forecast the FRP's long-term behaviour. Such an accelerated process speeds up the environmental aging process by taking advantage of the coupling effects formed by temperature and moisture [1,15]. It is the presence of extra thermal energy from an elevated temperature that enhances molecular mobility and accelerates the rate of degradation compared to what would be experienced under field conditions.

This paper reports experimental findings of an extensive investigation regarding the effects of moisture uptake on an 'off-the-shelf' PFRP material (flat-sheet) as part of the EPSRC funded DURACOMP project called 'Providing Confidence in Durable Composites' (EP/K026925/1). Samples were immersed in distilled water at four different constant temperatures of 25 °C, 40 °C, 60 °C and 80 °C for up to 224 days, following the test methodology of Bank et al. [1]. Moisture uptake characteristics were determined by a complementary investigation involving moisture uptake tests on both fully exposed (i.e. all six surfaces unsealed) and selectively exposed (i.e. four surfaces sealed) type of samples. Different sample dimensions were examined and their dimensional effects on the uptake behaviour are discussed. It was found that, different sample sizes and geometries significantly affect the results. Three different approaches involving Fickian theory were used to calculate diffusion coefficients. Fully, and selectively exposed samples were employed to calculate bulk and directional diffusion coefficients, respectively. In addition, electrical measurements and Fourier Transform Infrared Spectroscopy (FTIR) were employed to study the water uptake effects occurring due to hot/wet aging. The infrared spectrums of the un-aged PFRP and the water medium (residual substitutes) were analyzed and discussed. Scanning Electron Microscopy (SEM) and Energy Dispersive Spectroscopic (EDS) analyses assisted in the determination of the source of chemical decomposition found to cause substantial mass loss.

2. Accelerated aging and moisture uptake in FRPs

Long-term assessment of a material's durability in a short and realistic period of time (i.e. one year) could be experimentally feasible by applying accelerated aging. The process requires hygrothermal exposure and relies on the superposition of temperature and moisture to enhance and speed up environmental degradation. In order for accelerated aging to provide a realistic prediction of long-term service behaviour, the maximum exposure temperature according to Bank et al. [1] has to be lower, by i.e. 20 °C, than the polymer's glass transition temperature, T_g. It is recognized that secondary (and unwanted) degradation mechanisms will become activated when the exposure temperature approaches or exceeds T_g, and under this conditioning the accelerated aging fails to simulate the required aging process for field applications [8,15]. The degree of hygrothermal degradation is known to depend on the temperature and its adjacency to the polymer's T_g. Research reported by Surathi et al. [8]. shows that the higher the exposure temperature the higher is the moisture uptake rate and saturation content, as a consequence, the FRP reaches moisture saturation in shorter time periods than it can do so under field conditions.

Several theoretical approaches to modeling the moisture uptake process have been proposed [8,17,18]. From the many, Fick's theory is frequently reported for its suitability in determining moisture

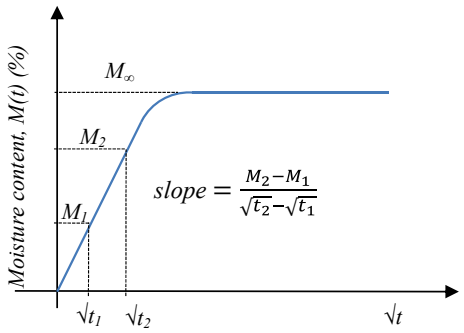

Fig. 1. Representative of a classical Fickian diffusion three-stage curve for $M(t)$ vs. $\sqrt{t}$.

diffusion coefficient [8]. A typical three-stage moisture uptake curve for the classical Fickian diffusion model is shown in Fig. 1. The ordinate axis is for $M(t)$, in percentages of original mass, and the abscissa is for square root of time. In the figure M_1 and M_2 are for moisture masses at times t_1 and t_2 in the linear range, respectively, and M_∞ is the maximum (saturation) moisture content. As can be seen in the figure, $M(t)$ starts to increase linearly with time. After this first initial stage which is at about 0.6 of the maximum, the rate of moisture uptake decreases gradually until it reaches the asymptotic constant equilibrium value (M_∞). In the case of a partially cured polymer matrix, this behaviour is altered and more stages might be encountered [8,19–22]. This deviation from the classical Fickian behaviour is known to mainly be caused by polymer relaxation [23]. After prolonged exposure beyond the time for the equilibrium state, certain polymer systems are known to start losing mass due to chemical degradation. In such case, there is an additional stage in the curve which is for a lowering in $M(t)$ after 'equilibrium'. This mass loss is mainly caused by decomposition of the low-molecular weight constituents leading to leaching of species (ions) into the water medium [24–27]. In addition to partial resin polymerization, aging temperatures close to T_g will further induce a deviation from the classical Fickian behaviour illustrated in Fig. 1 [21,28].

Moisture sorption and diffusion processes are functions of immersion temperature, the type of the polymer matrix, fibre orientation, fibre volume fraction and the space inside the material's structure that is not occupied with polymer molecules (i.e. free volume, porosity and micro-cracks). Assuming that classical Fickian diffusion takes place, moisture diffusion coefficient may be calculated from the initial linear part of the moisture uptake curve shown in Fig. 1. The slope of the linear part is given by:

$$Slope = \frac{M_2 - M_1}{\sqrt{t_2} - \sqrt{t_1}} \quad (1)$$

For classical Fickian behaviour the bulk coefficient D is a constant property with respect to moisture concentration and exposure temperature. Prolonged exposure induces a deviation from the classical Fickian process and diffusion is then non-Fickian [6,29]. In general, when a FRP sample, is exposed to aqueous media, moisture penetrates all six exposed surfaces. Moisture travels into the volume via the two main mechanisms of diffusion through the polymer matrix and capillary action ('wicking') along the fibre/matrix interface regions.

Before presenting test results it is important to understand that moisture ingress is more effective when the space which is free of polymer molecules in the volume of a FRP material is higher. This space usually corresponds to more of the FRP's volume having 'free volume' that can be occupied by water molecules penetrating in. Increasing temperature can cause physical changes to the molecular structure leading to a different amount of 'free volume' [9].

In the field, moisture ingress into a FRP structure will occur mainly through the material thickness and for this situation the one-dimensional (1D) Fickian model [8] is appropriate to model moisture uptake. Edge effects (moisture ingress through the four edge surface areas (or cross-section edges)) may have a negligible effect on uptake in relation to absorption via the other two (larger) surfaces in the plane of the material. This 'large' structures behaviour is not the case in laboratory testing where relatively small size samples are used. As a consequence of a size effect our contribution examines the effect of different relative geometrical ratios on the moisture uptake characteristics. The above postulation raised the necessity to investigate the use of selectively exposed samples with only two of the six surfaces allowing moisture uptake in order to be able to establish the directional (orthogonal) diffusion characteristics in the three principal axes i.e. D_x, D_y and D_z.

3. Material

The characterization work was conducted on a commercially available PFRP flat sheet (FS040.101.096A (1/4″ × 48″ × 96″/Series 1500 (I))) supplied by Creative Pultrusions Inc. (http://www.creativepultrusions.com/). The nominal thickness of the flat sheet was 6.4 mm, composed of isophthalic polyester matrix and E-glass fibre reinforcement. Fig. 2 displays that the structure of the PFRP material consists of three Continuous Strand Mat (CSM) layers with a 33.3% volume fraction of fibres and two UniDirectional (UD) layers with an average 54.5% volume fraction of fibres.

The outer surfaces of the flat sheet are covered by an additional protecting thin (~25–40 μm thickness) and non-structural polyester veil, which has the dual functions of retarding moisture ingress and protecting the PFRP material from UV radiation. It is worth mentioning that after moisture penetrates pass the outermost veil layer it is free to travel in the longitudinal and transverse directions; being fastest parallel to the UD fibres. It can be postulated that the veil (surface) area/edge (cross-section) area ratio and the relative magnitudes of the directional diffusion coefficients play a significant role in the moisture uptake characteristics when samples are fully exposed to the aqueous medium. For the PFRP flat sheet, coefficients in the through-thickness (D_z) and transverse (D_x) directions can be expected to be lower than in the longitudinal (pultrusion or 'fibre') direction (D_y).

Table 1 details the shapes and sizes of the samples cut from the flat sheet using a water-cooled diamond saw. Column (1) introduces the unsealed and sealed samples and column (2) gives their plan shape. In column (3) the first six rows define the plan (side length) dimensions for the square or rectangular shapes. The bottom three rows are for the sealed samples that have a nominally 6.4 mm thickness in either of the x, y or z principal directions (Fig. 3). The corresponding constant immersion temperatures employed for hot/wet aging are listed in column (4). As aforementioned, two different types of samples were examined: (i) fully exposed (unsealed); and (ii) selectively exposed (with either the through-thickness (z-direction), the longitudinal (y-direction) or the transverse (x-direction) edges exposed). For type (i) the samples have square or rectangular shape. Type (ii) samples possess identical size and geometry with moisture uptake allowed in only a single principal direction. Figs. 3(a)–(c) show these three constant-sized samples. To fabricate the longitudinal and transverse (edge exposed) samples in Fig. 3(b) and (c) four layers of the 6.4 mm thick sheet were bonded together with a cyanoacrylate superglue having negligible bondline thickness. Figs. 3(a)–(c) show a schematic representation of the selectively exposed samples with reference to the pultrusion (UD) direction and the principal (x, y, z) axes. In Fig. 3(a) the area exposed is for uptake in the through-thickness direction (z-axis). As Fig. 3(b) and (c) show these samples have exposed surface areas for moisture movement in the transverse (x-axis) and longitudinal (y-axis) directions, respectively. Samples were prepared in a way that exposed an opposing pair of edge surfaces that are perpendicular to the direction of moisture uptake being characterized. To ensure a 100% barrier to moisture an epoxy layer and aluminum tape layer of ~30 μm thickness were applied to the four non-exposed surfaces. The thickness of the epoxy was <1 mm in order to minimize moisture uptake in this layer that inherently leads to confusion with the recorded moisture uptake data. The developed test configuration is expected to make negligible the amount of moisture absorbed by the epoxy layer and aluminum tape volumes [30].

A thorough investigation on batch variation is not given in this

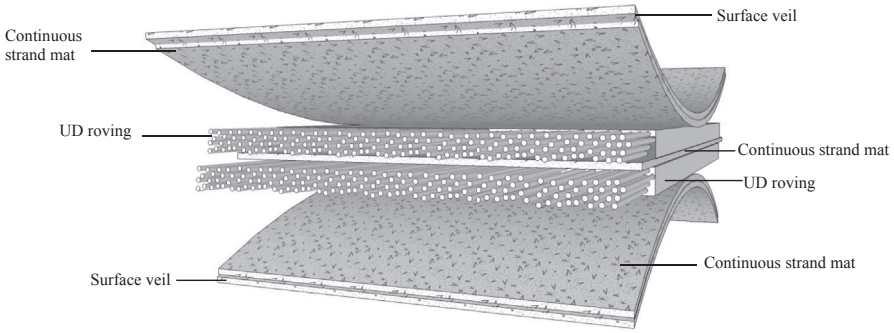

Fig. 2. Construction of the five layered PFRP flat sheet material.

Table 1
Samples and corresponding aging temperatures.

(1)	Sample type (2)	Dimensions (3)	Temperature/°C (4)
Fully exposed (unsealed)	Square	40 × 40 mm^2	25, 40, 60, 80
		80 × 80 mm^2	25, 40, 60, 80
		200 × 200 mm^2	25, 40, 60, 80
	Rectangular	50 × 70 mm^2	60
		70 × 50 mm^2	60
		25 × 250 mm^2	60
Selectively exposed (edge/face sealed)	Through-thickness edge exposed	71 × 25.6 × 6.4 mm^3	60
	Transverse edge exposed	71 × 6.4 × 25.6 mm^3	60
	Longitudinal edge exposed	6.4 × 71 × 25.6 mm^3	60

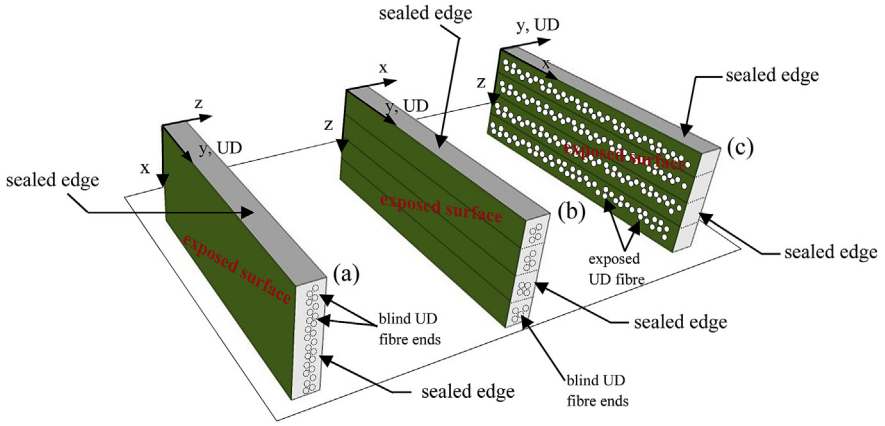

Fig. 3. Schematic configuration of the selectively exposed samples: (a) through-thickness edge exposed (z-axis direction, veil surface); (b) transverse edge exposed (x-axis direction); (c) longitudinal edge exposed (y-axis direction).

paper owing to lack of space and because the testing had to be carried out with batches of one or more nominally identical samples. For batches having five samples a statistical analysis based on the Gaussian distribution showed that the batch variation was low enough (~2–4% CV) to allow for the assumption that a single sample result can be considered as presenting the nominal value for the population mean.

4. Experimental procedure

4.1. Moisture uptake

After samples were sized they were oven-dried at 30 °C for 48 h in order to start with complete dryness. They were weighed using a digital analytical scale having ±0.001 mg sensitivity. After immersion in distilled water in the temperature-controlled water tanks (SUB36, Grant, UK) the samples were removed at pre-determined times in order to measure their moisture 'uptake'. The relative moisture change ($M(\%)$) for a sample was determined using Equ. (2), taken from ASTM D 5229:

$$M(\%) = \frac{M_t - M_0}{M_0} \times 100\% \quad (2)$$

where M_t is the measured 'moisture' mass at time t and M_o is the initial mass at the dry state. Moisture uptake measurements were conducted over a time period of 224 days [1]. For the calculation of moisture diffusion coefficient, Fickian theory is commonly employed assuming uniform moisture and temperature conditions

throughout the volume. Fick's transient equation is:

$$\frac{\partial z}{\partial t} = D\frac{\partial^2 C}{\partial z^2} \tag{3}$$

where z is the distance into the thickness (h) from an exposed surface, C is the concentration of water and D is the bulk diffusion coefficient (mm^2/s) [29]. In this work, bulk diffusion coefficient refers to the case of fully exposed samples. Crank [29] develops the summation solution to Equ. (3) as:

$$\frac{M_t}{M_\infty} = 1 - \frac{8}{\pi^2}\sum_{k=0}^{\infty}\frac{1}{(2k+1)^2}\exp\left(-\frac{D(2k+1)^2\pi^2 t}{h^2}\right) \tag{4}$$

Equ. (4) can be simplified for short- and long-term time approximations as:

$$\frac{M_t}{M_\infty} = \frac{4}{\pi^2}\sqrt{\frac{Dt}{h^2}} \quad \text{for} \quad Dt/h^2 < 0.04 \tag{5}$$

and

$$\frac{M_t}{M_\infty} = 1 - \frac{8}{\pi^2}\exp\left(\frac{-Dt}{h^2}\pi^2\right) \quad \text{for} \quad Dt/h^2 > 0.04 \tag{6}$$

As long as M_∞ can be established from a gravimetric curve (Fig. 1), D for a statistical homogeneous material can be determined using the following expression and two points of the moisture uptake M_1 and M_2 at times t_1 and t_2:

$$D = \pi\left(\frac{h}{4M_\infty}\right)^2\left(\frac{M_2 - M_1}{\sqrt{t_2} - \sqrt{t_1}}\right)^2\left(1 + \frac{h}{l} + \frac{h}{w}\right)^{-2} \tag{7}$$

Parameters l and w are for the length and width of a sample. In Equ. (7) moisture diffusion is assumed to occur mostly in the thickness direction (one-dimensional/1D). The last dimensional factor of the equation represents the effect of the edges [6] that can be neglected in the case of the selectively exposed samples of this study. In order to calculate the principal diffusion coefficients of D_x, D_y and D_z from the unsealed (fully exposed) samples, a methodology initially reported by Shen et al. [6], and later by Pierron et al. [31] was followed. These researchers assumed that for the linear part of the moisture sorption curve one can approximate a three-dimensional behaviour by:

$$D = D_z\left(\frac{h}{l}\sqrt{\frac{D_y}{D_z}} + \frac{h}{w}\sqrt{\frac{D_x}{D_z}} + 1\right)^2 \tag{8}$$

where D is the bulk moisture diffusion coefficient that can be determined by Equ. (7). Individual calculations of D_x, D_y and D_z are feasible if there are test results from three samples having different aspect ratios of side lengths, with a constant h.

For the purpose of this study, bulk (fully exposed samples) and directional (fully and selectively exposed samples) diffusion coefficients were calculated using Equs. (7) and (8). Directional coefficients were determined for samples aged at 60 °C, since this constant temperature is the most effective. To achieve the same results at the aging temperatures of 25 °C and 40 °C would require a significantly extended period of time for the 6.4 mm PFRP material to reach moisture saturation. Accelerated aging at 80 °C was found to be very aggressive, enabling secondary degradation mechanisms to be activated, leading to substantial mass loss.

4.2. Electrical properties

The electrical properties of the water medium at 60 °C were monitored by means of electrical conductivity, pH and total dissolved solids. For these measurements a 'pH & water analysis meter' (Hanna Instruments, UK) was used.

4.3. Fourier transform infrared spectroscopy

Samples of the water medium at the 60 °C were selectively collected from the water tank and oven-dried. The remaining substances were studied using a Fourier Infrared spectrometer with a view to identifying their chemical structure. The spectra derived for the water substances were compared with spectra of the un-aged material. Matrix material was first separated from the glass fibers before samples were scanned in the range of 500 cm^{-1} to 4000 cm^{-1}, using a Perkin Elmer Frontier spectrometer equipped with a diamond MIRacle ATR (Pike) and using a DGTS detector with KBr optics.

4.4. Scanning electron microscopy and energy dispersive spectroscopy

Scanning Electron Microscopy (SEM) and Energy Dispersive Spectroscopic (EDS) analyses were used to further investigate the microstructure of the water substances and to identify the chemical elements that are in the bulk aged and un-aged matrix. An JSM-6480LV (JEOL, Japan) SEM was adopted to collect images under variable pressure mode at 60 Pa to alleviate charging that would impair the imaging quality.

5. Results and discussion

This section is split into the two sub-sections to cover the moisture uptake behaviour (5.1) and the chemical decomposition (5.2) found throughout the aging process.

5.1. Moisture uptake

Plotted in Fig. 4(a)–(d) are single-sample curves for moisture uptake results as a function of time (t) for the fully exposed square samples (listed at the top of Table 1). The abscissa axis has a linear scale for t in days. The ordinate axis is for M as a percentage of the original sample mass (M_o) in Equ. (2), and in parts (a) to (d) it ranges from 0 to 3%. Because of the substantial mass loss when aging at 80 °C the ordinate scale of Fig. 4(d) has a negative part to −1.5%. In the four parts (a) to (d) there are three curves coloured: light green (triangle symbol) for smallest sample size 40 × 40 mm^2; light blue (square symbol) for size 80 × 80 mm^2; dark blue (diamond symbol) for largest size 200 × 200 mm^2. It is observed that the initial rate of moisture uptake increases with increasing immersion temperature from 25 °C in Fig. 4(a) to 80 °C in Fig. 4(d). Based on the plots it can be seen that no sample at 25 °C (Fig. 4(a)) and 40 °C (Fig. 4(b)) had reached the moisture saturation state, after 224 days, whereas those immersed in distilled water at 60 °C (Fig. 4(c)) reached saturation after approximately 140 days. The three 80 °C curves in Fig. 4(d) show that a 'saturation time' of 40 days is about one-quarter that at 60 °C.

It is evident from the graphical representation in Fig. 4 that by increasing the aging temperature results in:

(i) increased moisture content (M(%));
(ii) higher moisture uptake rate;
(iii) reduced number of days to reach equilibrium (M_∞).

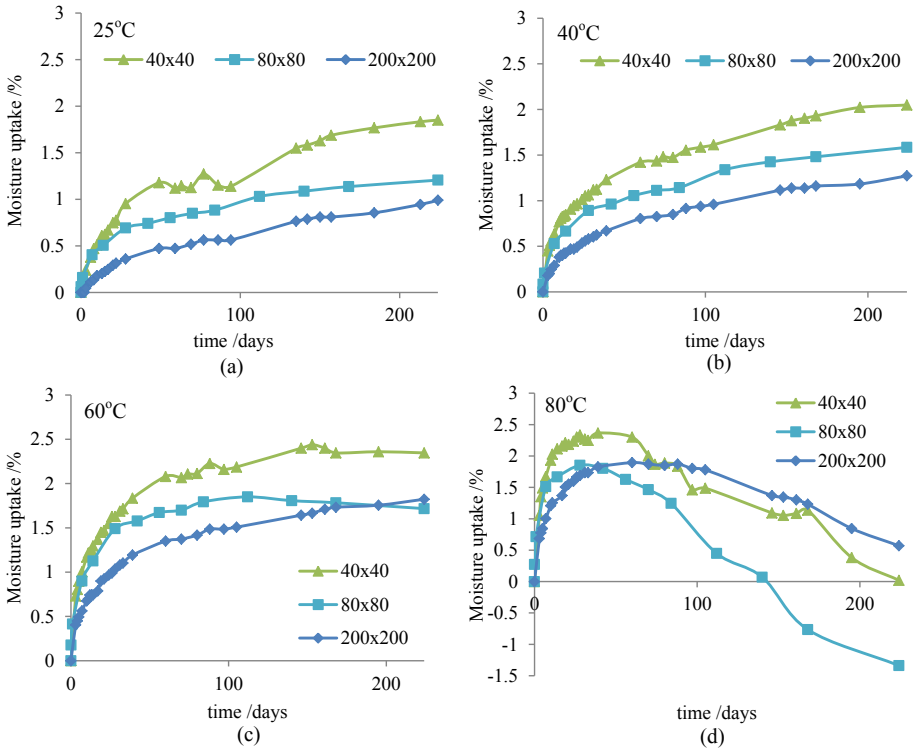

Fig. 4. Plots for percentage mass moisture uptake with time in days: (a) 25 °C; (b) 40 °C; (c) 60 °C; (d) 80 °C.

On the assumption that the limit of moisture uptake is not temperature dependent, it is possible that M_∞ at the two lowest immersion temperatures could be equal or similar to what is measured at i.e. 60 °C. Based on the work of Chin et al. [32] it could take up to a few years for a FRP material to reach moisture saturation at 40 °C or lower temperature. The uptake trend in Fig. 4(d) presents a characteristic behaviour different of that presented in Figs. 4(a) to 4(c). After M_∞ is reached there is a decrease in mass, at a virtually constant rate, indicating that uptake is less effective than mass loss of PFRP material into the water medium [33]. The decomposition phenomenon observed is thoroughly analyzed in Sub-Section 5.2.

Fig. 5(a) and (b) present the same results for the samples of plan sizes 40 × 40 mm^2 and 200 × 200 mm^2 at the four immersion temperatures. The solid lines for the experimentally derived curves were modelled by Fickian theory using Equ. (6) to construct the dashed lined curves. Using the curves in Figs. 4 and 5 it is found that at 25 °C, 40 °C and 60 °C the moisture uptake process for the PFRP flat sheet material does follow a classical Fickian trend. As already alluded to, there is a dramatic deviation from Fickian behaviour at 80 °C owing to significant and irreversible mass loss. A size dependency is clearly one manifestation from the test results presented in Fig. 5(a) and (b). As expected, the smallest sample size of 40 × 40 mm^2 required fewer days to reach saturation at 60 °C and 80 °C. This may be attributed to the relative difference in the amount of 'free volume'; that is because the smaller sized samples possess quantitatively less 'free volume', voiding and microcracking, and hence less overall distance for the moisture to travel.

Columns (2) to (4) in Table 2 report M_∞ and D values, as well as the veil area/edge area ratios for the three square sample sizes given in column (1). The bulk diffusion coefficients are calculated using Eq. (7). M_{max} is also taken, for our convenience, to be M_∞ for the samples that had not reached equilibrium at the end of the aging regime (e.g. the 200 × 200 mm^2 samples aged at 25 °C). To

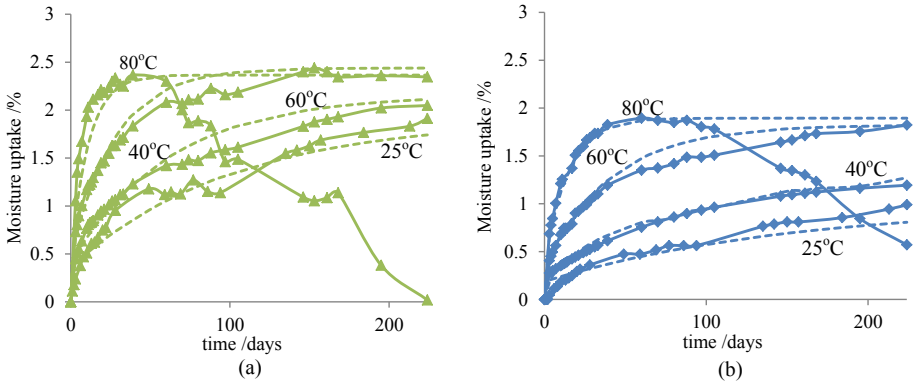

Fig. 5. M(%) with t for the four temperatures: (a) 40 × 40 mm^2; (b) 200 × 200 mm^2.

Table 2
Maximum moisture contents, bulk diffusion coefficients and the veil area/edge area ratios for the fully exposed square samples.

Side dimensions (mm^3) (1)	M_∞ (%) (2)				D ($\times 10^{-6}$ mm^2/s) (3)				Veil area/edge area (4)
	25 °C	40 °C	60 °C	80 °C	25 °C	40 °C	60 °C	80 °C	
40 × 40 × 6.4	1.85	2.04	2.34	2.49	0.47	0.77	1.60	4.25	3.12
80 × 80 × 6.4	1.20	1.58	1.85	1.80	0.81	0.19	2.34	6.60	6.25
200 × 200 × 6.4	0.98	1.27	1.82	1.89	0.42	0.52	1.15	3.26	15.6

explain the meaning of the veil area/edge area ratio, the ratio for sample size 40 × 40 mm^2 will be developed. There are two (plan) surfaces with a continuous veil layer and, as they are 40 × 40 mm^2, the 'veil area' is 3200 mm^2. Since there are four edge surfaces, each having rectangular shape of 40 × 6.4 mm^2, the total 'edge area' is 1024 mm^2. The veil area/edge area ratio of 3.12 in column (4) is obtained from the division of 3200/1024. Results in the table for M_∞ and D are listed with respect to the four aging temperatures.

The curves in Figs. 4 and 5 exhibit a difference of approximately 1% in moisture uptake mass between the 40 × 40 mm^2 and 200 × 200 mm^2 samples. Because this finding enhances our initial postulation that there could be a sample size dependency it is logical to start the discussion on the test results by considering the influence of size.

The veil area/edge area ratio can be used to quantify the relative amount of moisture uptake occurring in the through thickness z-direction with respect to uptake occurring through the edge surfaces that are in the longitudinal y-direction and transverse x-direction. As the plan side lengths increase, so does the veil area/edge area ratio and this leads to a decrease in M_∞. Taking the 60 °C results in column (2) of Table 2, M_∞ is 2.34% for the smallest and 1.82% for the largest sample size. As mentioned previously in the paper this sample-size difference changes the time taken for the PFRP material to reach moisture saturation.

It is found that the PFRP material undergoes chemical decomposition with mass loss as part of the aging process, which is most significant at 80 °C (Fig. 4(d)). It will be shown in Sub-Section 5.2 that mass loss is active after the very first days of immersion with highest rate for the smallest sized sample. This observation can be associated to the veil area/edge area ratio, which at 3.12 for size 40 × 40 mm^2 is five times lower than for sample size of 200 × 200 mm^2. An outcome of this observation is that material adjacent to the longitudinal and transverse edge surfaces must be decomposing at a higher rate than material adjacent to the much greater 'veil' surface areas. As seen from the curves in Fig. 4(d) this size difference leads to a higher mass loss after 224 days. The higher amount of moisture content reported in column (2) of Table 2 with the 40 × 40 mm^2 sample size might be explained by the following mechanism: the smaller the sample size is, the lower will be the amount of 'free volume', voiding and micro-cracking, and hence less soaking time is required to reach M_∞. This indicates that there is relatively less distance to be covered by water molecules to create the saturation state. Results indicate that after 224 days the majority of the 40 × 40 mm^2 samples (see Fig. 5(a)) had reached saturation, even if M_∞ is not stable because of chemical decomposition. In contrast, saturation in 224 days for the 200 × 200 mm^2 size could only be reached at 80 °C (see Fig. 5(b)). By accepting that moisture diffusion is going to be most rapid over the longitudinal and transverse edge surfaces we observe that the smaller the veil area/edge area ratio is, the quicker will be the time for the sample to reach moisture saturation. All the above discussion, based on the test results from the fully exposed square samples, is pointing to the fact that the determined bulk diffusion coefficients using a Fickian formula will vary with sample size.

This observation is supported by the varying D values reported in column (3) of Table 2. For the four hot/wet immersion temperatures the range for the bulk diffusion coefficients using Equ. (7) ranges between 0.19 × 10^{-6} and 6.60 × 10^{-6} mm^2/s. As expected from the physics of moisture uptake, the tabulated D values are seen to be higher as the aging temperature increases. Interestingly, it is found that the three square sample sizes gave a different diffusion coefficient at each aging temperature. The highest and lowest D of the 16 is found to be established from the test results of the 80 × 80 mm^2 samples. Although this finding, again, indicate a size effect, it does not assist with offering a physical explanation. The authors can speculate that D in the narrower range of 0.42–3.26 × 10^{-6} mm^2/s from the largest sample size is closer to the actual bulk material diffusion coefficient. This is because there is little edge surface influence; the moisture ingress via the six surfaces interacts less during the early stages of the moisture uptake process. Furthermore, the bulk diffusion coefficient determined from 40 × 40 mm^2 samples is expected to be higher than that determined from the larger samples. The effect of significant relative mass loss with the 40 × 40 mm^2 size is the reason, at temperatures of 40 °C, 60 °C and 80 °C, for the higher D values in column (2) of Table 2. As a consequence of the unreliability in using the smallest sample authors do not recommend using sample sizes in moisture uptake characterization that have a low veil area/edge area ratio; currently there are insufficient test results to specify a pragmatic minimum ratio.

In order to overcome the size-dependency effect it was decided to conduct testing with the selectively exposed samples whose sizes are defined in the bottom three rows of Table 1. Using the outcomes from the fully exposed square samples this part of the characterization work was at the single immersion temperature of 60 °C. Samples were now sealed such that only one pair of faces could be exposed for moisture uptake. In order to provide a fair comparison between the diffusivities in the three principal directions, the selectively exposed samples had to satisfy the following criteria (see Fig. 3):

(a) identical exposed area (71 × 25.6 mm^2 here);
(b) identical volume (71 × 25.6 × 6.4 mm^3 here);
(c) identical moisture-travelling path lengths (6.4 mm here).

Failure to meet any one of the three criteria is likely to affect dramatically the moisture uptake rate, M_∞ and the time to saturation, and be detrimental to a strong comparison between the results from the three selectively exposed-samples.

Table 3 presents the diffusion coefficients corresponding to the principal directions in the PFRP material. Fig. 3 shows that subscript y is for the longitudinal direction that is parallel to the UD fibre reinforcement, x is for transverse direction and z is for the through-thickness direction. Equ. (7) was, again, employed, without taking into account the last dimensional parameter to correct for the edge effects. As expected, the descending order in magnitudes of the principal diffusion coefficients are D_y = 9.26 × 10^{-6} $mm^2/s > D_x$ = 7.04 × 10^{-6} $mm^2/s > D_z$ = 1.85 × 10^{-6} mm^2/s. D_z is for the

Table 3
Principal (directional) diffusion coefficients for the PFRP 6.4 mm thick flat sheet material.

Directional diffusion coefficient ($\times 10^{-6}$ mm^2/s) at 60 °C		
Selectively sealed samples		
D_x	D_y	D_z
7.04	9.26	1.85

through-thickness uptake and is seen to be very close to the three *D*s of 1.15 $\times$ 10^{-6} to 2.34 $\times$ 10^{-6} mm^2/s for 60 °C in Table 2. The slight difference can be associated with the edge effects in the case of the fully exposed samples.

For the selectively exposed condition, Fig. 6 plots the uptake with time (for a single sample situation). The orange curve with square symbols is for moisture uptake in the *x*-direction (transverse edge exposed, shown in Fig. 3(b)). For the direction in the plane and parallel to the UD reinforcement the *y*-direction uptake curve (for longitudinal edge exposure in Fig. 3(c)) is green with solid triangular symbols. The third curve with light blue rhombus symbols is for the *z*-direction (through-thickness edge) characteristics. As can be seen from the curves in Fig. 6 the uptake rate is highest in the longitudinal direction. It is seen that it is the *z*-direction sample that saturates with the highest M_∞, and this finding is expected, thereby enhancing our postulations regarding the influence on uptake on the veil area/edge area ratio. The impact of this key ratio on uptake is important since a veil surface impedes diffusion of moisture into the body of the material. This factor is not present for the cross-section edge exposed samples were uptake is seen to be rapid. As well as creating a barrier to diffusion the veil surface is less susceptible to chemical decomposition than the four edge surfaces. As a consequence it is found that the lower the veil area/edge area ratio is the more mass loss is recorded. This provided an explanation to why there is a higher M_∞ with the *z*-direction sample. The three uptake curves presented in Fig. 6 show that there is a noticeable difference in moisture uptake behaviour because the PFRP material has surfaces with the thin polyester veil.

In the third and final part of this diffusion, the rectangular fully exposed samples introduced in Table 1 were employed for the determination of the principal diffusion coefficients. The 3D approximation proposed by Shen et al. [6] was applied with test results from three samples having different side length aspect ratios. Moisture uptake was recorded until M_∞ was reached for the rectangular shapes defined in rows four to six of Table 1. Using Equ. (7), and the same data reduction procedure as with the square fully exposed samples, three diffusion coefficients were determined for the three rectangular sizes. The simplification to the analysis enables the principal values D_x, D_y and D_z to be computed from a 3 $\times$ 3 matrix formed on using Equ. (8). Listed in columns (1) to (6) of Table 4 are the input properties required to calculate the principal coefficients reported in columns (7) to (9). D_z at 0.55 $\times$ 10^{-6} mm^2/s and D_y at 45 $\times$ 10^{-6} mm^2/s are an order of magnitude different to the equivalent diffusion coefficients of 1.85 $\times$ 10^{-6} mm^2/s (significantly higher) and 9.26 $\times$ 10^{-6} mm^2/s (significantly lower), respectively, which were determined from testing the selectively exposed edge samples of Table 1. It is noted that the two D_xs of 5.3 $\times$ 10^{-6} mm^2/s (Table 4) and 7.8 $\times$ 10^{-6} mm^2/s (Table 3) are not too different. It is well understood that differences in *D* values can be attributed to the differences in test methodology, as well as the assumptions involved in the mathematical approximation employed for their determination, as reported in Table (4). Since the principle on which we apply Equ. 8 is that the samples possess different geometrical aspect ratios, it may be presumed that testing with a significantly higher difference in side length aspect ratios would provide a more reliable determination of the diffusion coefficients.

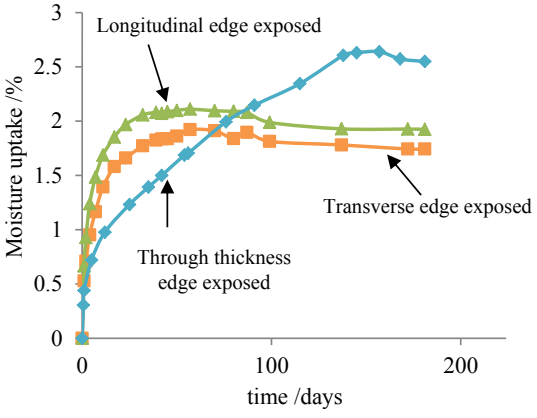

Fig. 6. Moisture uptake (%) with time for the selectively exposed samples at 60 °C.

5.2. Chemical decomposition

For the reasons discussed in Sub-Section 5.1 the curves plotted in Figs. 4 to 6 do not reflect the true moisture uptake as the recorded mass change with time is the superposition of uptake and mass loss [26,33]. Chemical decomposition of an FRP is a crucial feature in moisture diffusion characteristics, especially when the aging temperature is relatively high, e.g. 20 °C below the material's T_g [1]. Prolonged aging leads to physical and chemical degradation such as plasticization, hydrolysis, etc. The onset of decomposition complicates the interpretation of the gravimetric readings as the ('Fickian') real water uptake process is masked by the weight decrease. Depending on the exposure temperature, the decomposition process could initiate at different soaking times after immersion. In this work, the decomposition phenomenon of the PFRP flat sheet material was studied for the 60 °C aging temperature.

In order to assess the occurrence of decomposition, the water medium was initially investigated by means of electrical properties. Nine PFRP samples of plan size of 25 $\times$ 25 mm^2 were immersed in 400 ml of distilled water at 60 °C inside a sealed beaker. Throughout an exposure time of 224 days the pH, the Electrical Conductivity (EC) and the Total Dissolved Solids (TDS) were recorded and the results are plotted in Fig. 7. As seen from the curve with square symbols a reduction in pH is mirrored by an increase in both EC (curve with rhombus symbols) and TDS (curve with triangle symbols). These results reveal that decomposition must have initiated in <7 days of immersion, and that hydrolysis is allowing ion-leaching into the water medium to increase the solution's EC [24,25]. Thus, elevation of the water's EC can be linked to an increase in ions released through hydrolysis of low molecular weight components in the polyester-based matrix. The pH of the solution has a decreasing tendency to being more acid, reaching, after 40 + days an asymptotic value of approximately 4. TDS increase denotes the presence of an increasing amount of solids (leachates) released into the original distilled water. The observable changes in pH, TDS and EC, as reported in Fig. 7, correspond to overall PFRP material decomposition [24,25,27]. Interestingly, the asymptotic trends with the three curves in the figure do suggest that either the dissolution rate is reducing or the solution is becoming saturated with ions and this allows the decomposition to slow down. These general observations indicate that a comprehensive understanding of the decomposition process requires a deeper investigation.

Liquid samples were collected for chemical examination. Fig. 8 is

Table 4
Fully exposed rectangular samples aged at 60 °C; bulk and principal diffusion coefficients using the three-dimensional approximation from Shen et al. [6].

Moisture uptake at equilibrium (%)			Bulk (total) diffusion coefficient ($\times 10^{-6}$ mm^2/s)			Directional diffusion coefficient ($\times 10^{-6}$ mm^2/s)		
(1)	(2)	(3)	(4)	(5)	(6)	(7)	(8)	(9)
M_∞ (250 × 50 mm^2)	M_∞ (50 × 70 mm^2)	M_∞ (70 × 50 mm^2)	D (250 × 50 mm^2)	D (50 × 70 mm^2)	D (70 × 50 mm^2)	D_x	D_y	D_z
1.76	1.84	1.67	2.26	2.72	3.28	5.26	44.8	0.55

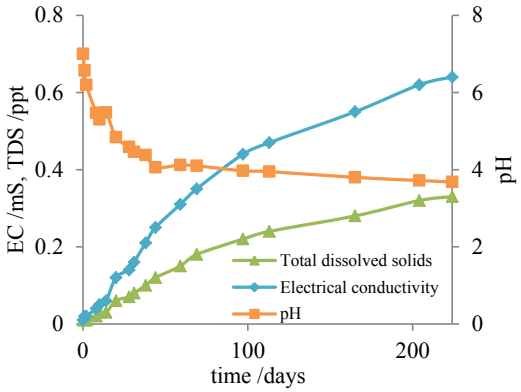

Fig. 7. pH, EC and TDS as mass is lost during hot/wet aging in original distilled water at 60 °C.

a schematic presentation of the experiment to characterize the wet-aging of the PFRP at 60 °C. Fig. 8(a) is the set-up at zero days and Fig. 8(b) shows what substances are released in the distilled water after 224 days. Part (b) shows that there are three fractions which correspond to mass loss, comprising material that is: floating; suspended; flocculated. These fractions were collected separately and oven-dried. After drying it was obvious that the substances left were from PFRP decomposition.

All three substances were subjected to FTIR with the view to determining their chemical compositions and origins. For reference purposes, an un-aged sample was scanned and its spectrum compared with those of the substances. Matrix fractions from the as-received material were separated from the E-glass fibre reinforcement to prepare the samples. The plotting in Fig. 9 is a juxtaposition of the un-aged material (top) and the three water substances (in order from top to bottom) of floating, suspended and flocculated materials. To the right of the four plots in Fig. 9 is a sequence of SEM micrographs of the three water substances that were floating, suspended and flocculated.

The peaks in the infrared spectra of Fig. 9 demonstrate organic vibrations associated with the polyester resin in the un-aged state. Basic assignments include a broad peak owing to the presence of O–H depicted in the region of 3400 cm^{-1}. The broad peak sets at around 2930 cm^{-1} might be attributed to C–H stretching. A weak peak at 1730 cm^{-1} indicates the presence of ester groups (carboxyl acid groups). Peaks at 1580 and 1403 cm^{-1} correspond to carboxylate stretching, whereas the peak at 1090 cm^{-1} is due to O–H bending. The basic representative peaks of the polymer are at 1077 cm^{-1} and 1031 cm^{-1} which correspond to silica and unreacted matrix, respectively. Overall, the FTIR spectrum, which is similar to that reported by Chin et al. [32], allows for the notion of chemical decomposition since the residues include chemical groups from the polyester matrix. The main part of the substances in solution is of polyester with evidence of oxidation damage. There is also a significant amount of silica present. Using the results in Fig. 7 it is known that decomposition initiates almost immediately after immersion and can be speculated that providing the water does not reach saturation it continues until the entire accessible chemical groups are consumed.

Fig. 10 depicts two micrographs of matrix fractured surfaces for a reference (un-aged) sample and an aged sample at 60 °C for 224 days. The micrographs clearly show the 'fibre-pockets' or the areas where the fibres were enclosed before fracture. As is pointed on the images, there is a fibre–fibre interface area which consists of a matrix phase that is found in-between the reinforcing fibres. It is obvious from both micrographs in Fig. 10(a) and (b) that there are 'air gaps' or 'air pockets' that remained inside the 'fibre-pocket' areas after the detachment of the fibres. These clusters-like 'air pockets' can be attributed to the fibre sizing or fillers that were used to enhance fibre/matrix bonding. The images suggest that the fillers are left on the matrix part after fracture due to a 'weak' fibre/matrix interfacial bond with the fibres (Fig. 10(b)) which exhibit a smooth surface with no attached crystals. Polyester resins are known to be susceptible to acid attack, which in this study is formed by the low pH solution [34]. From SEM observations of fractured surfaces (Fig. 10) it is proposed that the fibre sizing (coupling agent) has been selectively removed after aging and/or did not adequately couple the reinforcement and matrix together. This would suggest that during the pultrusion process the sizing had not been fully wetted by, or integrated with, the curing polymer, thereby allowing

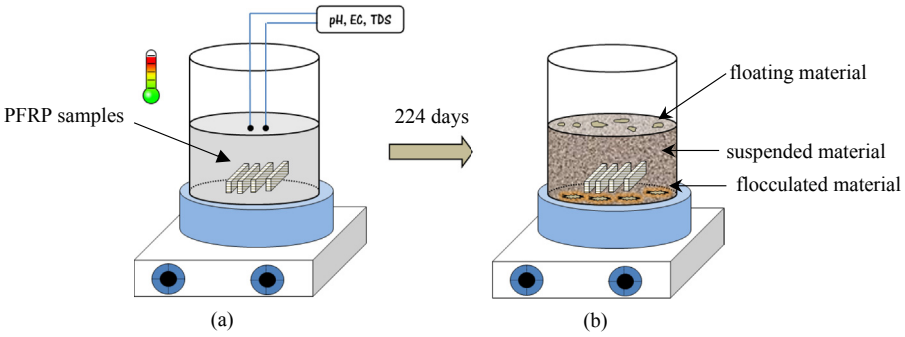

Fig. 8. Image representation of the PFRP decomposition process at 60 °C. (a) pure distilled water at zero days, (b) water substances leached in the solution after 224 days.

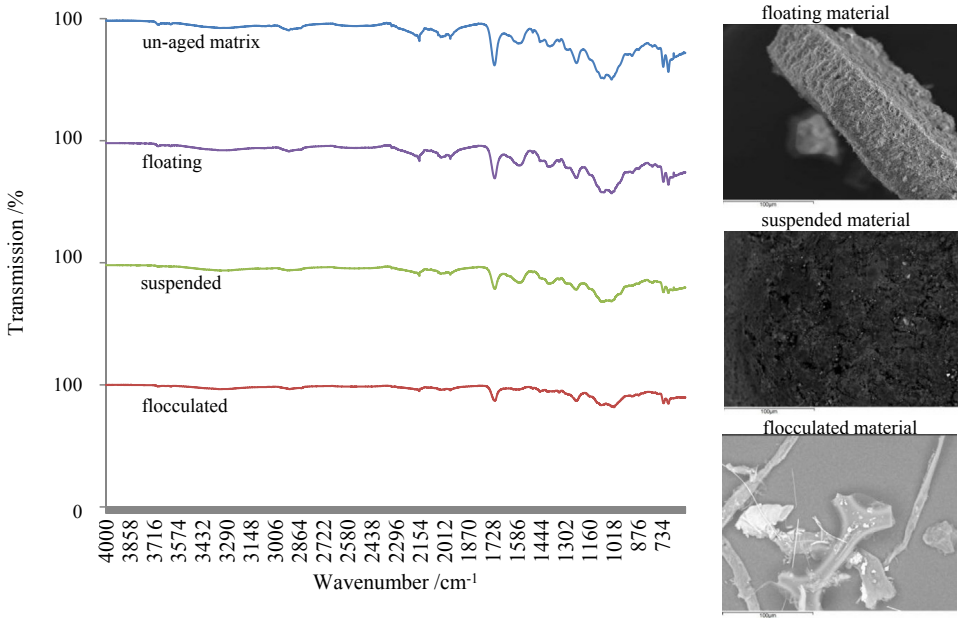

Fig. 9. FTIR spectra for (from top to bottom) the: un-aged matrix, floating, suspended and flocculated materials.

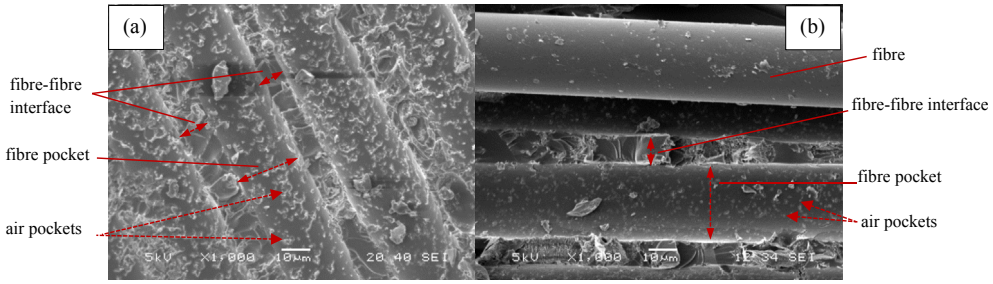

Fig. 10. SEM micrographs of fractured matrix surfaces: (a) un-aged; (b) after aging at 60 °C for 224 days.

some of the silica-based sizing to be readily removed during the aging process. The remaining silica-based sizing that with the matrix has formed the interphase region does not have the same properties as the bulk matrix; the hydroscopic nature of SiO_2 and the presence of moisture from the environment cause the sizing being partially impregnated and thus preventing from uniform curing. This weaker matrix (inter) phase is more prone to acid attack and so the outcome is that small silica particles connected to resin dissolve, and disperse, into the 'suspended' water medium (Fig. 8). The heavier silica containing poorly cured resin flocculates at the bottom of the beaker and the more buoyant cured resin floats. This fragmentation of material going into the solution is due to the lamella nature of the PFRP flat sheet.

In addition, Energy Dispersive Spectroscopy (EDS) was used to identify the chemical elements present in all samples collected from the aging baths shown in Fig. 8. This analysis reinforces the proposed mechanisms of dissolution outlined by evaluation of the FTIR results in Fig. 9. The suspended material contains a significant amount of free silica and the floating material contains oxygen-poor polymer. In the flocculated material there is presence of silica and mineral particles in high quantities along with oxygen rich resin indicating oxidation. A typical EDS spectrum is given in Fig. 11 for the un-aged material. EDS analysis of the water substances reveals, along with carbon (C) and oxygen (O) from the polymer, the presence of Cl^-, Na^+, SO_2^-, SO_3^-, Al^{3+}, Ca^{2+}, Mg^{2+}, Zn^+, etc., which correspond to the 'total dissolved solids' that led to the increase of electrical conductivity (see Fig. 7) of the water medium. Previous studies revealed negligible hygrothermal degradation of the fibre reinforcement which was less significant than the degradation of the matrix and fibre/matrix interface [35]. The fibre/matrix interface/interphase is expected to show a high degradation rate exposing the reinforcement to moisture attack. EDS elemental analysis of the fibre reinforcement of samples at the un-aged and aged states as shown in Table 5, indicates insignificant surface chemical changes after hygrothermal aging.

As can be seen in the micrograph attached in Fig. 11 there are bright areas in the image for where there is a concentration of heavy elements, such as Al, Si, etc. The darker areas correspond to the polymer matrix formed of principally carbon and oxygen.

The interpretation of the FTIR and EDS scans is difficult and challenging because details of the constituents and processing of the 'off-the-shelf' pultruded material are not in the public domain. The pultruder Creative Pultrusion Inc. (USA) use a matrix, in % mass, consisting of 75.3% Reichold 31-031 polyester resin, 15.1% clay, 4.5% styrene and the other 6.1% of eight constituents required in the pultrusion composite processing. To that end, this inhibited the quantification of the water substances.

5.3. Mass loss after drying

Table 6 reports the percentage of mass loss after 224 days from a selection of three sample sizes and all investigated immersion

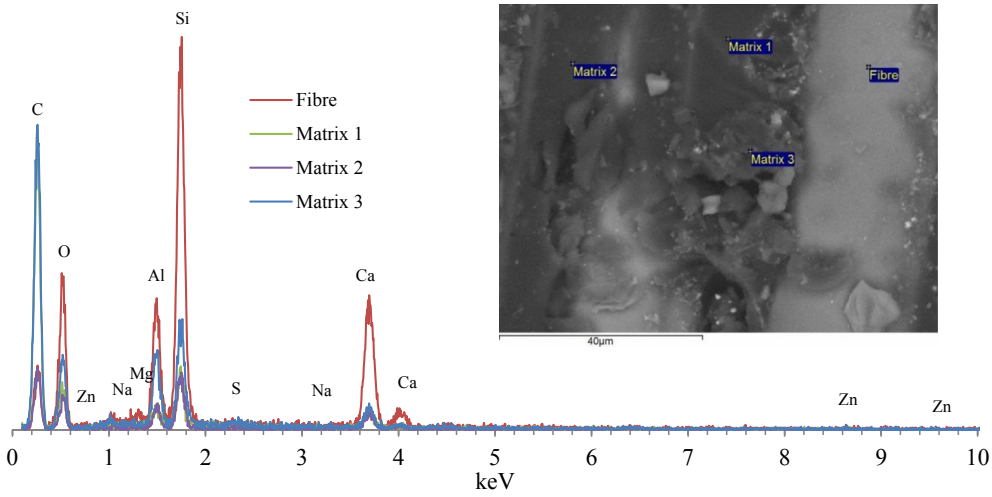

Fig. 11. Typical EDS spectra and a SEM micrograph for the un-aged material.

Table 5
Percentage weight composition of glass fibre reinforcement for the un-aged and aged states.

	Percentage weight composition (%)						
	C	O	Mg	Al	Si	Ca	Total
Reference (un-aged)	26.48	43.34	0.49	4.69	15.86	9.14	100
Aged at 60 °C for 224 days	27.64	41.3	0.41	4.81	16.89	8.95	100

Table 6
Mass loss due to hygrothermal aging after drying.

Mass loss (%) of their initial dry mass				
Dimensions (mm^3)	25 °C	40 °C	60 °C	80 °C
40 × 40 × 6.4	0.24	0.34	1.00	5.3
80 × 80 × 6.4	0.26	0.29	0.86	4.0
200 × 200 × 6.4	0.27	0.98	0.79	3.7

temperatures. Samples were oven-dried at the same temperature that was used for their aging (i.e. if hot/wet aged at 40 °C, oven dried at 40 °C) for a period of approximately 20 days or until their weight was stabilized at a constant value ensuring that the samples are completely dry.

Fig. 12(a) is a graphical representation of the change in moisture uptake of the FRP material over a prolonged time period. The characteristic curve can be divided into the following three distinct stages:

i. In stage (I) moisture uptake and material decomposition are competing until the condition of moisture saturation is reached. During this stage uptake rate is greater than mass loss.
ii. During stage (II) moisture uptake has reached a maximum or its rate of increase is equal or less than the rate of mass loss into the immersion solution.
iii. In stage (III) the decomposition rate is dominant. (To establish actual mass loss an aged sample can be dried.)

Fig. 12(b) shows the effect of the veil area/edge area ratio on moisture content at saturation and on mass loss for the case of the square samples aged at 60 °C for 224 days. As can be seen, increasing the ratio leads to both a lower M_∞ and lower mass loss. This is evidence to support the abovementioned observation and principal diffusion coefficients that the four edge surface areas absorb moisture at higher rates than the two (larger) surfaces with an outer veil layer. At the same time, the material close to the edges areas is more prone to chemical deterioration after moisture penetrates the internal structure, thereby activating dissolution of the composite. Interfacial loss enhances the moisture wicking along the

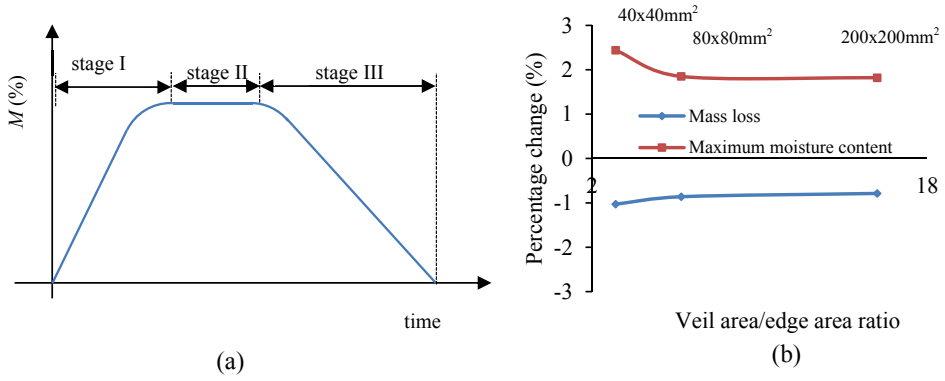

Fig. 12. (a) Schematic configuration of a moisture uptake curve as a function of time; (b) effect of veil area/edge area ratio on M_∞ and mass loss for the three square sample sizes aged at 60 °C for 224 days.

fibre reinforcement. One finding from the characterization work on moisture uptake of the PFRP flat sheet is that, even after moisture penetrates past the protective veil, this thin, non-structural layer, is continuing to provide a degree of sorption protection to the internal structure the material.

6. Concluding remarks

Moisture uptake characteristics of a Pultruded E-glass Fibre Reinforced Polymer (PFRP) material have been investigated throughout hot/wet aging of fully (unsealed) and selectively exposed (sealed) samples of a 6.4 mm thick flat sheet. Mass changes with time from both types of samples have been employed to determine bulk and principal (directional) diffusion coefficients. The three different approaches, based on Fickian modeling, used to calculate coefficients are:

1. one-dimensional Fickian approximation for bulk diffusion coefficient (at 25 °C, 40 °C, 60 °C and 80 °C) for the fully exposed samples of square shape;
2. one-dimensional Fickian approximation for principal coefficients (at only 60 °C) for the selectively exposed samples;
3. three-dimensional Fickian approximation for principal coefficients (at only 60 °C) employing a set of fully exposed rectangular samples having different side length aspect ratios.

A variety of supplementary analysis methodologies were employed to study in-depth the moisture uptake characteristics. Electrical measurements, Fourier Transform InfraRed Spectroscopy (FTIR) and Energy Dispersive Spectroscopy (EDS) were undertaken to investigate the substances leached into solution from chemical decomposition of the PFRP material. This comparative study with fully and selectively exposed samples has enhanced our knowledge on the response of a particular E-glass fibre and isophthalic polyester matrix composite exposed to environmental aging.

In particular, it is observed that:

- hot/wet aging accelerates the maximum moisture content, uptake rate and time to saturation; the mass uptake at saturation is found to be influenced by mass loss from chemical decomposition.
- different sizes and geometries of the samples significantly affect the moisture uptake results and for the large sample sizes and low temperatures the 224 days study can be insufficient to reach the saturation condition.
- relatively small sized samples reach moisture saturation in less time than relatively larger ones and this is attributed to lower veil area/edge area ratio and a lower amount of free volume to be occupied by water molecules.
- the directional diffusion coefficient in the longitudinal (pultrusion) direction is higher than in the transverse and through-thickness principal directions.
- it is practical to determine the directional diffusion coefficients by having selectively exposed samples that satisfy specific dimensional criteria.
- determined directional diffusion coefficients varied for the different approaches owing to different test methodologies.
- veil protected surfaces impede, but do not stop the moisture uptake process; the veil is found to inhibit mass loss.
- the electrical property measurements revealed that dissolution initiated within the first days of hot/wet aging for samples aged at 60 °C.
- the FTIR spectra uncovered the origin of the leachates found in the water medium after aging
- the EDS spectra revealed the chemical signature of the leachates detached during aging.
- after 224 days there is a mass loss of 0.24–1.0% at temperatures of 25 °C–60 °C, increasing significantly to 3.7 and 5.3% at 80 °C.
- veil area/edge area ratio increase leads to both lower percentage mass uptake and mass loss over the aging period.

Finally, it is summarized that special care needs to be taken by computational modelers when developing analysis for such non-linear moisture uptake response of polymeric composites in aqueous environments because the behaviour of a FRP material is highly dependent on its processing and composition [36].

Acknowledgments

The work is part of the EPSRC funded project DuraComp (Providing Confidence in Durable Composites, EP/K026925/1).

References

[1] L.C. Bank, T.R. Gentry, A. Barkatt, Accelerated test methods to determine the long-term behavior of frp composite structures: environmental effects, J. Reinf. Plastics Compos. 14 (1995) 559–587.
[2] K.V. Pochiraju, G.P. Tandon, G.A. Schoeppner, Long-Term Durability of Polymeric Matrix Composites, Springer, 2011.
[3] S. Luke, L. Canning, S. Collins, E. Knudsen, P. Brown, B. Taljsten, et al., Advanced composite bridge decking system—project ASSET, Struct. Eng. Int. 12 (2002) 76–79.
[4] Maro Polymer Notes: Maro Communications; 1999.
[5] Y. Shao, S. Kouadio, Durability of fiberglass composite sheet piles in water, J. Compos. Constr. 6 (2002) 280–287.
[6] C.-H. Shen, G.S. Springer, Moisture absorption and desorption of composite materials, J. Compos. Mater. 10 (1976) 2–20.
[7] S. Cabral-Fonseca, J.R. Correia, M.P. Rodrigues, F.A. Branco, Artificial accelerated ageing of GFRP pultruded profiles made of polyester and vinylester resins: characterisation of physical–chemical and mechanical damage, Strain 48 (2012) 162–173.
[8] P. Surathi, V.M. Karbhari, Project SSR, University of California SDDoSE, Services CDoTDoE, Hygrothermal Effects on Durability and Moisture Kinetics of Fiber-reinforced Polymer Composites, Department of Structural Engineering, University of California, San Diego, 2006.
[9] O. Starkova, S.T. Buschhorn, E. Mannov, K. Schulte, A. Aniskevich, Water transport in epoxy/MWCNT composites, Eur. Polym. J. 49 (2013) 2138–2148.
[10] G.A. Schoeppner, G.P. Tandon, K.V. Pochiraju, Predicting thermooxidative degradation and performance of high-temperature polymer matrix composites, in: Y. Kwon, D. Allen, R. Talreja (Eds.), Multiscale Modeling and Simulation of Composite Materials and Structures, Springer US, 2008, pp. 359–462.
[11] J. Hinkley, J. Connell, Resin systems and chemistry: degradation mechanisms and durability, in: K.V. Pochiraju, G.P. Tandon, G.A. Schoeppner (Eds.), Long-Term Durability of Polymeric Matrix Composites, Springer US, 2012, pp. 1–37.
[12] Y. Joliff, L. Belec, M.B. Heman, J.F. Chailan, Experimental, analytical and numerical study of water diffusion in unidirectional composite materials – Interphase impact, Comput. Mater. Sci. 64 (2012) 141–145.
[13] M. Akay, S.K. Ah Mun, A. Stanley, Influence of moisture on the thermal and mechanical properties of autoclaved and oven-cured Kevlar-49/epoxy laminates, Compos. Sci. Technol. 57 (1997) 565–571.
[14] H. Ben Daly, H. Ben Brahim, N. Hfaied, M. Harchay, R. Boukhili, Investigation of water absorption in pultruded composites containing fillers and low profile additives, Polym. Compos. 28 (2007) 355–364.
[15] A.S. Maxwell, W.R. Broughton, G. Dean, G. Sims, Review of accelerated ageing methods and lifetime prediction techniques for polymeric materials, Natl. Phys. Lab. (2005). ISSN:1744-0270, NPL Doc. Ref:PDB:3915.
[16] B. Zafari, J.T. Mottram, Effect of hot-wet aging on the pin-bearing strength of a pultruded material with polyester matrix, J. Compos. Constr. 16 (2012) 340–352.
[17] T.C. Wong, L.J. Broutman, Water in epoxy resins Part II. Diffusion mechanism, Polym. Eng. Sci. 25 (1985) 529–534.
[18] H.G. Carter, K.G. Kibler, Langmuir-type model for anomalous moisture diffusion in composite resins, J. Compos. Mater. 12 (1978) 118–131.
[19] M.S. Tillman, B.S. Hayes, J.C. Seferis, Examination of interphase thermal property variance in glass fiber composites, Thermochim. Acta 392–393 (2002) 299–302.
[20] F.J. Johnson, W.M. Cross, D.A. Boyles, J.J. Kellar, "Complete" system monitoring of polymer matrix composites, Compos. Part A Appl. Sci. Manuf. 31 (2000) 959–968.
[21] S. Roy, Moisture-Induced Degradation, in: K.V. Pochiraju, G.P. Tandon, G.A. Schoeppner (Eds.), Long-term Durability of Polymeric Matrix Composites, Springer US, 2012, pp. 181–236.
[22] B. Dao, J.H. Hodgkin, J. Krstina, J. Mardel, W. Tian, Accelerated ageing versus

realistic ageing in aerospace composite materials. IV. Hot/wet ageing effects in a low temperature cure epoxy composite, J. Appl. Polym. Sci. 106 (2007) 4264–4276.
[23] A.R. Berens, Analysis of transport behavior in polymer powders, J. Membr. Sci. 3 (1978) 247–264.
[24] A. Apicella, C. Migliaresi, L. Nicolais, L. Iaccarino, S. Roccotelli, The water ageing of unsaturated polyester-based composites: influence of resin chemical structure, Composites 14 (1983) 387–392.
[25] L. Prian, A. Barkatt, Degradation mechanism of fiber-reinforced plastics and its implications to prediction of long-term behavior, J. Mater. Sci. 34 (1999) 3977–3989.
[26] H.P. Abeysinghe, W. Edwards, G. Pritchard, G.J. Swampillai, Degradation of crosslinked resins in water and electrolyte solutions, Polymer 23 (1982) 1785–1790.
[27] A. Visco, V. Brancato, N. Campo, Degradation effects in polyester and vinyl ester resins induced by accelerated aging in seawater, J. Compos. Mater. 46 (2012) 2025–2040.
[28] A.R. Berens, H.B. Hopfenberg, Diffusion and relaxation in glassy polymer powders: 2. Separation of diffusion and relaxation parameters, Polymer 19 (1978) 489–496.
[29] J. Crank, The Mathematics of Diffusion, Clarendon Press, 1975.
[30] N.L. Post, F. Riebel, A. Zhou, T. Keller, S.W. Case, J.J. Lesko, Investigation of 3D moisture diffusion coefficients and damage in a pultruded E-glass/polyester structural composite, J. Compos. Mater. 43 (1) (2008) 75–96.
[31] F. Pierron, Y. Poirette, A. Vautrin, A novel procedure for identification of 3D moisture diffusion parameters on thick composites: theory, validation and experimental results, J. Compos. Mater. 36 (2002) 2219–2243.
[32] J.W. Chin, K. Aouadi, M.R. Haight, W.L. Hughes, T. Nguyen, Effects of water, salt solution and simulated concrete pore solution on the properties of composite matrix resins used in civil engineering applications, Polym. Compos. 22 (2001) 282–297.
[33] T. Morii, T. Tanimoto, H. Hamada, Z.-I. Maekawa, T. Hirano, K. Kiyosumi, Weight changes of a randomly orientated GRP panel in hot water, Compos. Sci. Technol. 49 (1993) 209–216.
[34] WILEY, Properties and Behavior of Polymers 1 ed, 2, Wiley, 2011.
[35] M.A. Sawpan, A.A. Mamun, P.G. Holdsworth, Long term durability of pultruded polymer composite rebar in concrete environment, Mater. Des. 57 (2014) 616–624.
[36] Y.J. Weitsman, M. Elahi, Effects of fluids on the deformation, strength and durability of polymeric composites – an overview, Mech. Time Dependent Mater. 4 (2000) 107–126.